

G.J. Lapeyre, Jr.,* M.D. Girardeau,† and E.M. Wright‡

Optical Sciences Center and Department of Physics, University of Arizona, Tucson, AZ 85721

(Dated: September 3, 2002)

Using the exact N -particle ground state wave function for a one-dimensional gas of hard-core bosons in a harmonic trap we develop an algorithm to compute the reduced single-particle density matrix and corresponding momentum distribution. Accurate numerical results are presented for up to $N = 8$ particles, and the momentum distributions are compared to a recent analytic approximation.

PACS numbers: 03.75.Fi, 03.75.-b, 05.30.Jp

I. INTRODUCTION

Recent advances in atom waveguide technology [1–10] and the realization of Bose-Einstein condensates in optical and magnetic traps of variable aspect ratio [11, 12] have spurred interest in the properties of degenerate quantum gases in lower dimensions. In particular, the Tonks gas, in which strong transverse confinement and low temperature and density allow the gas to be modeled as a one-dimensional (1D) system of point particles with hard-core interactions [13, 14], is of considerable theoretical interest due to the fact that it defies a mean-field description, but is on the other hand exactly soluble via the Fermi-Bose mapping [15, 16]. Although the exact many-body wave function can be written in a compact form using the mapping theorem, obtaining information about important observables has proven to be a difficult task. One such quantity that bears the signature of the Tonks gas is the momentum distribution, which has a sharp peak at zero momentum [13], in contrast to the Fermi sea for the corresponding 1D gas of fermions. In a mathematical *tour de force*, Lenard [17] obtained upper bounds on the momentum distribution for a homogeneous Tonks gas, and some elaborations of that work followed [18]. In a previous paper [19] we obtained numerical results for the momentum distribution of a harmonically trapped Tonks gas for up to $N = 10$ particles, and Minguzzi *et al.* [20] developed an analytic approximation for the high-momentum tail of the momentum distribution of a trapped gas. Cazalilla [21] obtained an analytic approximation for the momentum distribution of Tonks gas confined in a box using a description of the system as a Luttinger liquid.

Our previous calculations of a trapped Tonks gas were performed using a Monte Carlo (MC) integration of the many-body wave function to obtain the single-particle reduced density matrix from which the momentum distribution was obtained via Fourier transformation. Although the data thus generated were useful, an improved method is desirable because of the limited accuracy of MC integration. Even these MC data were limited to $N = 10$ particles, which required weeks of computer time. It seems clear that the way forward is to have high-precision numerical data available for testing the

validity of approximations. In this paper we start from the N -particle ground state wave function for a one-dimensional condensate of hard-core bosons in a harmonic trap and develop an algorithm to compute the reduced single-particle density matrix and momentum distribution. The key advantage of this approach is that, although we are limited to only $N = 8$ particles at present by computer resources, these data are of high precision, thus providing a testing ground for analytic approximations.

In Sec. II, we give a precise definition of the system and find the ground state wave function using the Fermi-Bose mapping theorem. In Sec. III, we write the single-particle reduced density matrix ρ_1 and develop a method for its numerical solution. In Sec. IV we use these results for ρ_1 to evaluate the momentum distribution and compare the results to a recent approximation for the high-momentum tail.

II. GROUND STATE WAVE FUNCTION

The Hamiltonian of N bosons in a 1D harmonic trap is

$$\hat{H} = \sum_{j=1}^N \left[-\frac{\hbar^2}{2m} \frac{\partial^2}{\partial \tilde{x}_j^2} + \frac{1}{2} m \omega^2 \tilde{x}_j^2 \right]. \quad (1)$$

We assume that the two-body interaction potential consists only of a hard-core of 1D diameter a . This is conveniently treated as a constraint on allowed wave functions $\tilde{\psi}(\tilde{x}_1, \dots, \tilde{x}_N)$ such that

$$\tilde{\psi} = 0 \quad \text{if} \quad |\tilde{x}_j - \tilde{x}_k| < a, \quad 1 \leq j < k \leq N, \quad (2)$$

rather than as an infinite interaction potential. It follows from the Fermi-Bose mapping theorem [15, 16, 22] that the exact N -boson ground state ψ_{B0} of the Hamiltonian (1) with the constraint (2) is

$$\tilde{\psi}_{B0}(\tilde{x}_1, \dots, \tilde{x}_N) = |\tilde{\psi}_{F0}(\tilde{x}_1, \dots, \tilde{x}_N)|, \quad (3)$$

where $\tilde{\psi}_{F0}$ is the ground state of a fictitious system of N spinless fermions with the same Hamiltonian (1) and constraint. At low densities it is sufficient [13, 14] to consider the case of impenetrable point particles, the zero-range limit $a \rightarrow 0$ of Eq. (2). Since wave functions of “spinless fermions” are antisymmetric under coordinate exchanges, their wave functions vanish automatically whenever any $\tilde{x}_j = \tilde{x}_k$, the constraint

*Electronic address: lapeyre@physics.arizona.edu

†Electronic address: girardeau@optics.arizona.edu

‡Electronic address: Ewan.Wright@optics.arizona.edu

has no effect, and the corresponding fermionic ground state is the ground state of the *ideal* gas of fermions, a Slater determinant of the lowest N single-particle eigenfunctions $\tilde{\phi}_n$ of the harmonic oscillator (HO)

$$\tilde{\psi}_{F0}(\tilde{x}_1, \dots, \tilde{x}_N) = \frac{1}{\sqrt{N!}} \det_{(n,j)=(0,1)}^{(N-1,N)} \tilde{\phi}_n(\tilde{x}_j). \quad (4)$$

The HO orbitals are

$$\tilde{\phi}_n(\tilde{x}) = \frac{1}{\pi^{1/4} x_{\text{osc}}^{1/2} \sqrt{2^n n!}} e^{-x^2/2} H_n(\tilde{x}/x_{\text{osc}}), \quad (5)$$

with $H_n(x)$ the Hermite polynomials and $x_{\text{osc}} = \sqrt{\hbar/m\omega}$ the ground state width of the harmonic trap for a single atom. For convenience, we introduce the dimensionless coordinates $x_i = \tilde{x}_i/x_{\text{osc}}$, and the corresponding ground state wave function ψ_{B0} . As we have shown in previous work [19], substitution of Eq. (5) into Eq. (4) and some matrix manipulations [23] lead to a simple but exact expression of the Bijl-Jastrow pair product form for the N -boson ground state:

$$\psi_{B0}(x_1, \dots, x_N) = C_N \left[\prod_{i=1}^N e^{-x_i^2/2} \right] \prod_{1 \leq j < k \leq N} |x_k - x_j|, \quad (6)$$

with normalization constant

$$C_N = 2^{N(N-1)/4} \left[N! \prod_{n=0}^{N-1} n! \sqrt{\pi} \right]^{-1/2}. \quad (7)$$

III. SINGLE-PARTICLE DENSITY MATRIX

A. Analytic formula

The reduced single-particle density matrix with normalization $\int \rho_1(x, x) dx = N$ for the ground state given by Eq. (6) is

$$\begin{aligned} \rho_1(x, x') &= N \int \psi_{B0}(x, x_2, \dots, x_N) \\ &\quad \times \psi_{B0}(x', x_2, \dots, x_N) dx_2 \cdots dx_N \\ &= \mathcal{N}_N e^{-x^2/2} e^{-x'^2/2} I(x, x'), \end{aligned} \quad (8)$$

where the integration is from $-\infty$ to ∞ for each coordinate unless otherwise stated, and

$$\mathcal{N}_N = N 2^{N(N-1)/2} \pi^{-N/2} \left[\prod_{n=0}^N n! \right]^{-1}, \quad (9)$$

and we have defined

$$\begin{aligned} I(x, x') &= \int \prod_{i=2}^N e^{-x_i^2} |x_i - x| |x_i - x'| \\ &\quad \times \prod_{2 \leq j < k \leq N} (x_k - x_j)^2 dx_2 \cdots dx_N. \end{aligned} \quad (10)$$

In the following subsection, we develop a method for analyzing $I(x, x')$. We will see that, when N is small enough (say 2 or 3), the exact expression is manageable, but that we must turn to numerical methods for larger N .

B. Numerical approach

The multidimensional integral (10) can be expressed in terms of polynomials, Gaussians, and error functions. But, even for relatively small N , the number of terms in such an expression is too large to be useful when written. We previously evaluated the reduced single-particle density matrix using MC methods [19], but with limited numerical accuracy. Here we present a seminumerical approach in which we represent the integral in terms of incomplete gamma functions and evaluate the result to machine precision for particular values of x and x' .

We reduce the integral $I(x, x')$ to incomplete gamma functions in the following way. Consider the case $x < x'$. We first integrate over x_2 , writing

$$\begin{aligned} I(x, x') &= \int dx_3 \cdots dx_N I_2 \prod_{i=3}^N e^{-x_i^2} |x_i - x| |x_i - x'| \\ &\quad \times \prod_{3 \leq j < k \leq N} (x_k - x_j)^2, \end{aligned} \quad (11)$$

where

$$\begin{aligned} I_2 &= I_2(x, x', x_3, \dots, x_N) \\ &= \left\{ \int_{-\infty}^x - \int_x^{x'} + \int_{x'}^{\infty} \right\} P_2 dx_2, \quad x' < x \end{aligned} \quad (12)$$

and

$$\begin{aligned} P_2 &= P_2(x, x', x_2, \dots, x_N) \\ &= e^{-x_2^2} (x_2 - x)(x_2 - x') \prod_{2 < k \leq N} (x_2 - x_k)^2. \end{aligned} \quad (13)$$

The integrand P_2 is an analytic function of x, x' , and x_2 (in the sense that derivatives of all orders in these variables exist), so that the integral over each of the three intervals is analytic in these variables. Furthermore, we can evaluate the integral over x_2 in Eq. (12) easily because the integrand is a Gaussian multiplied by a polynomial. We next integrate over x_3 , getting

$$\begin{aligned} I(x, x') &= \int dx_4 \cdots dx_N I_3 \prod_{i=4}^N e^{-x_i^2} |x_i - x| |x_i - x'| \\ &\quad \times \prod_{4 \leq j < k \leq N} (x_k - x_j)^2, \end{aligned} \quad (14)$$

where

$$\begin{aligned} I_3 &= I_3(x, x', x_4, \dots, x_N) \\ &= \left\{ \int_{-\infty}^x - \int_x^{x'} + \int_{x'}^{\infty} \right\} I_2 P_3 dx_3, \quad x' < x \end{aligned} \quad (15)$$

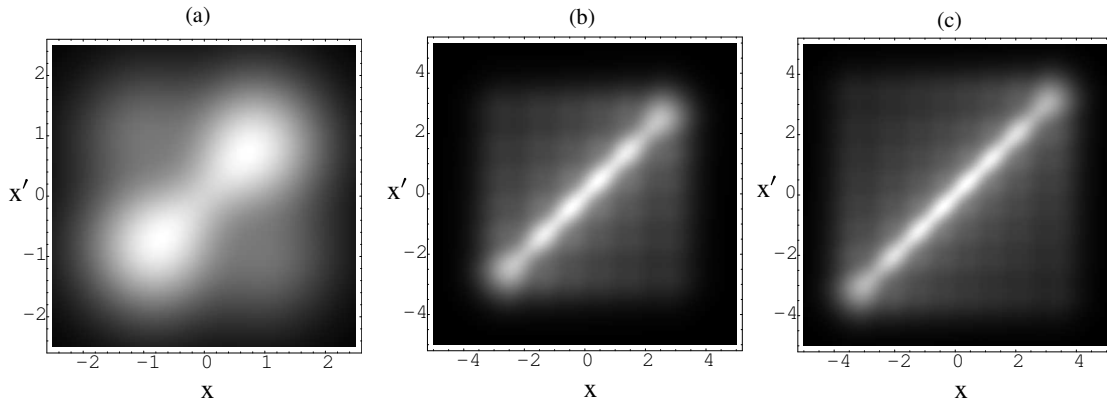


FIG. 1: Gray scale plots of the dimensionless reduced density matrix $x_{\text{osc}}\rho_1(x, x')$ as a function of the dimensionless coordinates x and x' , for (a) $N = 2$, (b) $N = 6$, and (c) $N = 8$.

and

$$P_3 = P_3(x, x', x_3, \dots, x_N) = e^{-x_3^2}(x_3 - x)(x_3 - x') \prod_{3 < k \leq N} (x_3 - x_k)^2. \quad (16)$$

It is important to note that, because I_2 is a polynomial in x_3, \dots, x_N , the integral I_3 in Eq. (15) can be solved by the same technique used to solve I_2 in Eq. (12). We continue this procedure, defining I_4 , etc., until all of the integrals are finished. At each stage, one has a more complicated polynomial in the remaining independent variables in the integrand. Before continuing, we note that there is, of course, nothing essentially new when we choose $x' < x$. For instance, for I_2 , we have

$$I_2 = \left\{ \int_{-\infty}^{x'} - \int_{x'}^x + \int_x^{\infty} \right\} P_2 dx_2, \quad x' < x. \quad (17)$$

If we examine each of the integrals I_2, I_3, \dots above, we see that all of the integrals to be computed can be reduced to terms proportional to integrals of the form

$$\alpha_n(x, x') = \left\{ \int_{-\infty}^x - \int_x^{x'} + \int_{x'}^{\infty} \right\} e^{-u^2} u^n du, \quad x < x' \quad (18)$$

and

$$\alpha_n(x, x') = \left\{ \int_{-\infty}^{x'} - \int_{x'}^x + \int_x^{\infty} \right\} e^{-u^2} u^n du \quad x > x'. \quad (19)$$

We now present an algorithm for expressing the integrals I_2, \dots in terms of the $\alpha_n(x, x')$ defined in Eqs. (18) and (19). To achieve this for I_2 , we take P_2 , drop the factor of $\exp(-x_2^2)$, expand the remaining factors as a polynomial in x_2 , and replace each occurrence of x_2^2 with $\alpha_n(x, x')$. The result is I_2 expressed as a polynomial in x, x', x_3, \dots with coefficients involving the $\alpha_n(x, x')$. This expression for I_2 is substituted into Eq. (15) and the same procedure is then used

to compute I_3 , and so on, until all powers of x_m^n have been replaced by $\alpha_n(x, x')$. This procedure can be simplified by performing all of these substitutions at once. To this end, consider

$$P = \prod_{i=2}^N (x_i - x)(x_i - x') \prod_{2 \leq j < k \leq N} (x_j - x_k)^2. \quad (20)$$

To compute the integral $I(x, x')$ given in Eq. (10), we expand Eq. (20) and substitute $\alpha_n(x, x')$ for each occurrence of x_m^n , for any m . In addition, for each value of m for which a term is independent of x_m , a factor of $\alpha_0(x, x')$ must be included. The result is $I(x, x')$ expressed as a polynomial in the $\alpha_n(x, x')$ for approximately $2N$ values of n . Rather than print the results, we store a table of the coefficients of the powers of $\alpha_n(x, x')$ on a computer. Then, a table of the $\alpha_n(x, x')$ is computed for a particular pair x, x' , and $I(x, x')$ is computed using this table together with the table of coefficients. Evaluating the $\alpha_n(x, x')$ using numerical integration is relatively inefficient. Instead, we evaluate them numerically using well-known, efficient routines to compute incomplete gamma functions. We define an indefinite integral

$$F_n(x) = \int e^{-x^2} x^n. \quad (21)$$

Then using definitions (18) and (19) we have

$$\alpha_n(x, x') = F_n(\infty) - F_n(-\infty) + \text{sgn}(x' - x) 2[F_n(x) - F_n(x')]. \quad (22)$$

$\alpha_n(x, x')$ is continuous, but has a cusp at $x = x'$. For numerical computation, we use

$$F_n(\infty) - F_n(-\infty) = \int_{-\infty}^{\infty} e^{-u^2} u^n = \begin{cases} 0 & \text{if } n \text{ is odd,} \\ \Gamma\left(\frac{1+n}{2}\right) = \sqrt{\pi} \frac{(n-1)!!}{2^{n/2}} & \text{otherwise,} \end{cases} \quad (23)$$

and

$$2[F_n(x) - F_n(x')] = [\text{sgn}(x)]^n \Gamma\left(\frac{1+n}{2}, x^2\right) - [\text{sgn}(x')]^n \Gamma\left(\frac{1+n}{2}, x'^2\right). \quad (24)$$

C. Examples

In this section we carry out in detail the algorithm given above for two particles and give the result for three particles. We first choose $N = 2$ and tabulate the required values of F_n and $\alpha_n(x, x')$. Integrating Eq. (21) by parts, we write

$$F_0(x) = \frac{\sqrt{\pi}}{2} \text{erf}x, \\ F_1(x) = -\frac{1}{2} e^{-x^2},$$

$$F_2(x) = \frac{1}{4} \sqrt{\pi} \text{erf}x - \frac{1}{2} x e^{-x^2}.$$

Using Eq. (22) we then have

$$\alpha_0(x, x') = \sqrt{\pi} + \text{sgn}(x' - x) \sqrt{\pi} (\text{erf}x - \text{erf}x'), \\ \alpha_1(x, x') = -\text{sgn}(x' - x) (e^{-x^2} - e^{-x'^2}), \\ \alpha_2(x, x') = \frac{\sqrt{\pi}}{2} + \text{sgn}(x' - x) \left[\frac{\sqrt{\pi}}{2} (\text{erf}x - \text{erf}x') + x' e^{-x^2} - x e^{-x'^2} \right].$$

Applying the algorithm outlined in the previous section we find for two particles

$$\rho_1(x, x') = \mathcal{N}_2 e^{-\frac{x^2}{2} - \frac{x'^2}{2}} \int_{-\infty}^{\infty} e^{-x_2^2} |(x_2 - x)(x_2 - x')| dx_2 = \mathcal{N}_2 e^{-\frac{x^2}{2} - \frac{x'^2}{2}} [\alpha_2(x, x') - (x + x')\alpha_1(x, x') + x x' \alpha_0(x, x')] \\ = \mathcal{N}_2 e^{-\frac{x^2}{2} - \frac{x'^2}{2}} \left\{ \sqrt{\pi} \left[\frac{1}{2} + x x' \right] + \text{sgn}(x' - x) \left[\left(\frac{1}{2} + x x' \right) \sqrt{\pi} (\text{erf}x - \text{erf}x') + x' e^{-x^2} - x e^{-x'^2} \right] \right\}.$$

For $N = 3$, one can easily compute the expression for $I(x, x')$ in terms of $\alpha_n(x, x')$ by hand, with the result

$$\rho_1(x, x') = 2\mathcal{N}_3 e^{-\frac{x^2}{2} - \frac{x'^2}{2}} \left\{ -\alpha_3^2 + \alpha_2 \alpha_4 + p^2 (-\alpha_2^2 + \alpha_1 \alpha_3) + t (\alpha_2^2 - 2\alpha_1 \alpha_3 + \alpha_0 \alpha_4) + t^2 (-\alpha_1^2 + \alpha_0 \alpha_2) + p [\alpha_2 \alpha_3 - \alpha_1 \alpha_4 + t (\alpha_1 \alpha_2 - \alpha_0 \alpha_3)] \right\},$$

where $p = x + x'$, $t = x x'$, and the explicit dependence of α_n on x and x' is omitted for clarity. For larger values of N , $I(x, x')$ rapidly becomes more difficult to compute by hand. In the next section we present the results of carrying out the algorithm detailed above on a computer.

D. Numerical results

We have evaluated the above integrals numerically for $N = 2-8$.

Figure 1 shows a gray scale plot of the dimensionless reduced single-particle density matrix $x_{\text{osc}} \rho_1(x, x')$ versus the normalized coordinates x and x' for (a) $N = 2$, (b) $N = 6$, and (c) $N = 8$. We verified that along the diagonal $\rho_1(x, x) = \rho(x)$ reproduced the single-particle density [24].

IV. MOMENTUM DISTRIBUTION

In terms of the boson annihilation and creation operators in position representation (quantized Bose field operators) the one-particle reduced density matrix is

$$\rho_1(x, x') = \langle \Psi_{B0} | \hat{\psi}^\dagger(x') \hat{\psi}(x) | \Psi_{B0} \rangle. \quad (25)$$

The momentum distribution function $n(k)$, normalized to $\int_{-\infty}^{\infty} n(k) dk = N$, is $n(k) = \langle \Psi_{B0} | \hat{a}^\dagger(k) \hat{a}(k) | \Psi_{B0} \rangle$ where $\hat{a}(k)$ is the annihilation operator for a boson with momentum $\hbar k$. Then

$$n(k) = (2\pi)^{-1} \int_{-\infty}^{\infty} dx \int_{-\infty}^{\infty} dx' \rho_1(x, x') e^{-ik(x-x')}. \quad (26)$$

The spectral representation of the density matrix then leads to $n(k) = \sum_j \lambda_j |\mu_j(k)|^2$ where the μ_j are Fourier transforms of the natural orbitals: $\mu_j(k) = (2\pi)^{-1/2} \int_{-\infty}^{\infty} \phi_n(x) e^{-ikx} dx$. Figure 2 shows the numerically calculated dimensionless momentum distribution $k_{\text{osc}} n(\kappa)$ versus normalized momentum $\kappa = k/k_{\text{osc}}$, with $k_{\text{osc}} = 2\pi/x_{\text{osc}}$, for (a) $N = 2$, (b) $N = 6$, and (c) $N = 8$. We typically evaluated $\rho_1(x, x')$ to machine precision for smaller values of κ , with precision decreasing to a part in 10^{-6} for the largest values of κ . The key features are that the momentum distribution maintains the peaked structure reminiscent of the spatially uniform case [13, 25] for the 1D HO, and that the peak becomes sharper with increasing

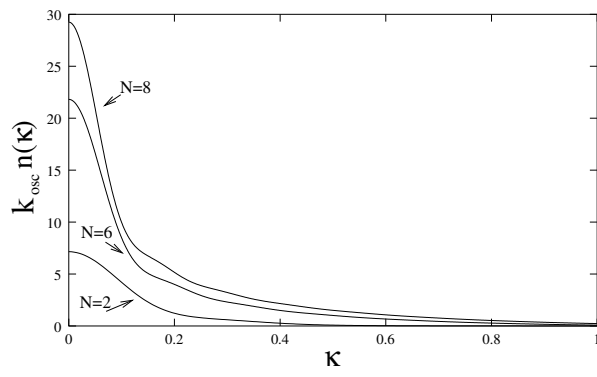


FIG. 2: Dimensionless momentum distribution $k_{\text{osc}}n(\kappa)$ versus normalized momentum $\kappa = k/k_{\text{osc}}$ for $N = 2$, $N = 6$, and $N = 8$. Note the peaks becoming sharper with increasing N .

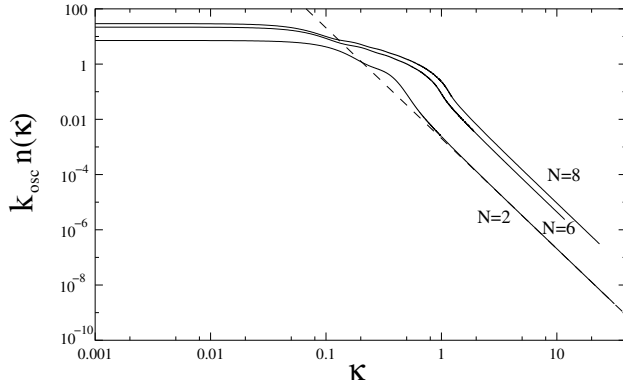


FIG. 3: Dimensionless momentum distribution $k_{\text{osc}}n(\kappa)$ versus normalized momentum $\kappa = k/k_{\text{osc}}$ on log-log scale. The dashed line is the asymptotic expression given by Eqs. (27) and (28).

atom number N . This is to be expected since as the number of atoms increases the many-body repulsion causes the system to become more spatially uniform within the trap interior. Minguzzi *et al.* [20] determined that the momentum distribution for finite N decays according to

$$\lim_{k \rightarrow \infty} k^4 n(k) = A_N, \quad (27)$$

where A_N depends only on the number of particles. In particular, for $N = 2$, they found

$$A_2 = 2\sqrt{\frac{2}{\pi}}(\hbar m \omega)^{-3/2}. \quad (28)$$

Figure 3 shows our numerical results for $N = 2$ approaching this asymptotic form. The dashed line in Fig. 3 shows $k_{\text{osc}}^5 A_2 / \kappa^4$ versus $\kappa = k/k_{\text{osc}}$, and we see that this approximation agrees with our numerical results for $N = 2$ for high momenta. Furthermore, inspection of the numerical results for other values of N shows a $1/k^4$ dependence in the high-momentum tail.

V. SUMMARY AND CONCLUSIONS

In summary, we have developed a method for obtaining high-accuracy results for the momentum distributions of trapped Tonks gases, and presented results for up to eight particles. Our results agree reasonably with the high-momentum approximation $n(p) \propto 1/p^4$ obtained by Minguzzi *et al.*

Acknowledgments

This work was supported by Office of Naval Research Grant No. N00014-99-1-0806 and the U.S. Army Research Office.

-
- [1] K. Bongs, S. Burger, S. Dettmer, D. Hellweg, J. Arlt, W. Ertmer, and K. Sengstock, *Phys. Rev. A* **63**, 031602 (2001).
 - [2] P. Cren, C. F. Roos, A. Aclan, J. Dalibard, and D. Guéry-Odelin, *Loading of a cold atomic beam into a magnetic guide* (2002).
 - [3] N. H. Dekker, C. S. Lee, V. Lorent, J. H. Thywissen, S. P. Smith, M. Drndic, R. M. Westervelt, and M. Prentiss, *Phys. Rev. Lett.* **84**, 1124 (2000).
 - [4] E. A. Hinds, M. G. Boshier, and I. G. Hughes, *Phys. Rev. Lett.* **80**, 645 (1998).
 - [5] M. Key, I. G. Hughes, W. Rooijackers, B. E. Sauer, and E. A. Hinds, *Phys. Rev. Lett.* **84**, 1371 (2000).
 - [6] A. E. Leanhardt, A. P. Chikkatur, D. Kielpinski, Y. Shin, T. L. Gustavson, W. Ketterle, and D. Pritchard, *Propagation of bose-einstein condensates in a magnetic waveguide* (2002), cond-mat/0203214.
 - [7] D. Müller, D. Z. Anderson, R. J. Grow, P. D. D. Schwindt, and E. A. Cornell, *Phys. Rev. Lett.* **83**, 5194 (1999).
 - [8] F. Schreck, L. Khaykovich, K. L. Corwin, G. Ferrari, T. Bourdel, J. Cubizolles, and C. Salomon, *Phys. Rev. Lett.* **87**, 080403 (2001).
 - [9] J. H. Thywissen, R. M. Westervelt, and M. Prentiss, *Phys. Rev. Lett.* **83**, 3762 (1999).
 - [10] M. Vengalattore, W. Rooijackers, and M. Prentiss, *Novel ferromagnetic atom waveguide with in situ loading* (2001), physics/0106028.
 - [11] A. Görlitz, J. M. Vogels, A. E. Leanhardt, C. Raman, T. L. Gustavson, J. R. Abo-Shaeer, A. P. Chikkatur, S. Gupta, S. Inouye, T. Rosenband, et al., *Phys. Rev. Lett.* **87**, 130402 (2001).
 - [12] M. Greiner, I. Bloch, O. Mandel, T. W. Hänsch, and T. Esslinger, *Phys. Rev. Lett.* **87**, 160405 (2001).
 - [13] M. Olshanii, *Phys. Rev. Lett.* **81**, 938 (1998).
 - [14] D. S. Petrov, G. V. Shlyapnikov, and J. T. M. Walraven, *Phys. Rev. Lett.* **85**, 3745 (2000).
 - [15] M. Girardeau, *J. Math. Phys.* **1**, 516 (1960).
 - [16] M. D. Girardeau, *Phys. Rev.* **139**, B500 (1965), see particularly Secs. II, III, and VI.
 - [17] A. Lenard, *J. Math. Phys.* **7**, 930 (1964).
 - [18] H. G. Vaidya and C. A. Tracy, *Phys. Rev. Lett.* **42**, 3 (1979).
 - [19] M. D. Girardeau, E. M. Wright, and J. M. Triscari, *Phys. Rev. A* **63**, 033601 (2001).

- [20] A. Minguzzi, P. Vignolo, and M. P. Tosi, Phys. Lett. A **294**, 222 (2002).
- [21] M. A. Cazalilla, *Low-energy properties of a one-dimensional system of interacting bosons with boundaries* (2002), cond-mat/020146.
- [22] M. D. Girardeau and E. M. Wright, Phys. Rev. Lett. **84**, 5691 (2000).
- [23] A. C. Aitken, *Determinants and Matrices* (Oliver and Boyd, Edinburgh and London, 1951), p. 112.
- [24] E. B. Kolomeisky, T. J. Newman, J. P. Straley, and X. Qi, Phys. Rev. Lett. **85**, 1146 (2000).
- [25] A. Lenard, J. Math. Phys. **7**, 1268 (1966).